Clays and Clay Minerals, Vol. 39, No. 2, 137–143, 1991.

EFFECTS OF IRON OXIDATION STATE ON THE TEXTURE AND STRUCTURAL ORDER OF Na-NONTRONITE GELS

JOSEPH W. STUCKI[1] AND DANIEL TESSIER[2]

[1] Department of Agronomy, University of Illinois, Urbana, Illinois, 61801

[2] Station de Science du Sol, INRA, Route de Saint Cyr, 78026 Versailles, France

Abstract—Aqueous gels of unaltered (oxidized) and chemically reduced ferruginous smectite (SWa-1 from the Source Clays Repository of The Clay Minerals Society) were characterized by transmission electron microscopy, electron diffraction, and energy-dispersive X-ray fluorescence to establish details regarding their texture, inter-layer and inter-particle arrangements, and chemical composition. Micrographs revealed that the reduction of structural Fe(III) to Fe(II) caused a consolidation of smectite particles from an extensive network of small crystals (1–6 layers thick) to distinct particles of limited size in the *a-b* direction and about 20–40 layers thick. The interlayer distances in the reduced sample appeared to be more uniform than in the oxidized sample, but both exhibited spacings of about 12.6 Å. Chemical analysis showed no qualitative differences as a result of oxidation state. Electron diffraction patterns displayed marked differences. The pattern of the oxidized sample consisted of homogeneous rings, indicating that the stacking order in the *a-b* plane was turbostratic or disordered, whereas the reduced pattern exhibited much more order as evidenced by distinct spots amid low-intensity rings, suggesting that inter-layer attractive forces were stronger if Fe(II) was present in the clay crystal.

Key Words—Electron diffraction, Ferric iron, Ferrous iron, High-resolution transmission electron microscopy, Layer structure, Nontronite.

INTRODUCTION

The chemical reduction of Fe(III) to Fe(II) in the crystal structure of smectite clay minerals greatly influences the chemical and physical properties of the clay (Stucki, 1988; Stucki and Lear, 1989), and several studies have suggested that many of these effects are related to changes in the face-to-face attractive forces between clay layers. Stucki *et al.* (1984b) and Lear and Stucki (1989) showed that the interlayer repulsive force in smectite, i.e., swelling in water, decreases with increasing Fe(II) content, and that the specific surface area, as measured by ethylene glycol-monoethylether adsorption, is greatly diminished. Chen *et al.* (1987), Lear and Stucki (1989), and Khaled and Stucki (1991) also observed a marked increase in the fixation of interlayer cations (Na^+, K^+, Ca^{2+}, Cu^{2+}, and Zn^{2+}) by the chemical reduction of structural Fe. X-ray powder diffraction (XRD) analysis of reduced and unaltered (oxidized) Na-nontronite gels revealed fewer fully expanded layers in the reduced than in the oxidized clay (Wu *et al.*, 1989), indicating that reduction imparts a more consolidated texture to the gel. All of these observations suggest that the face-to-face inter-layer attraction is greater in the reduced than in the oxidized smectite; some evidence, namely, increased cation fixation and decreased specific surface area, suggests that totally collapsed layers must also exist. But inasmuch as these measurements are only indirect with respect to clay texture and microstructure, except possibly for the XRD study of Wu *et al.* (1989), more direct measurements should be obtained if a complete understanding of the effects of Fe oxidation state on clay properties is to be developed.

Tessier (1984) showed that the organization of clay layers with respect to one another in aqueous smectite gels can be observed directly by high-resolution electron microscopy (HRTEM). Although he used Ca^{2+} as the interlayer cation, the same general principles should be applicable to Na-smectite. Analysis with a high-quality electron microscope also provides the added advantage of obtaining electron diffraction and elemental analyses, which are further direct measurements of crystal order and composition. The present study was undertaken to determine by HRTEM, electron diffraction, and elemental analysis the chemical composition and the inter-layer and inter-particle organization, i.e., the texture or microstructure, of Na-nontronite gels as affected by the oxidation state of Fe in the crystal structure.

MATERIALS AND METHODS

The clay used was the <2-μm fraction of ferruginous smectite SWa-1 (Source Clays Repository of The Clay Minerals Society), which was prepared as a Na-saturated and freeze-dried stock material. Reduced gels were prepared by suspending 100 mg of stock clay in 30 ml of citrate-bicarbonate buffer solution (Stucki *et al.*, 1984a), adding 100 mg of sodium dithionite ($Na_2S_2O_4$) salt, and heating at 70°C under an inert atmosphere in an open-system reaction vessel for 2 hr

(Komadel *et al.*, 1990), bringing the clay to about 50% reduction. The clay thus reduced was then washed by centrifugation to a solute concentration of about 10^{-4} N, and the suspension was placed in a pressure cell described by Stucki *et al.* (1984b) under 10 kPa N_2 gas pressure. Excess liquid was expelled from the sample through a porous membrane filter (0.025-μm pore diameter) at the bottom of the pressure cell, forming a clay gel on the membrane surface. An unaltered (oxidized) gel was prepared in like manner, except that no reducing agent ($Na_2S_2O_4$) was added.

Water in the clay gels was replaced by solvent exchange first with methanol (100% reagent) and then with medium grade LR White (LRW) resin (Ernest F. Fullam, Inc., Latham, New York), using a modification of the method of Tessier (1984) as follows. All solvents were degassed by imposing a modest vacuum while bubbling O_2-free N_2 gas. The pressure cell containing the equilibrated gel was carefully dismantled, and the gel was quickly cut into 3-mm-wide segments with a surgical scalpel. Care was taken to avoid using the outer fringes of the sample, which may have been distorted by the cell walls. Each segment was placed undisturbed inside a porous vial (7 × 7 mm); the vial was capped and then immersed in degassed, 100% methanol solution in a polypropylene bottle. After 2 and 4 hr of immersion, the vials were transferred to flasks containing freshly prepared methanol solutions and stored overnight in a refrigerator. The solvent was then changed to a mixture of methanol and LRW (1:2 v/v) at 0°C for 2 hr, and to pure LRW for 6 hr. In the last stage, the resin was changed every 2 hr. Samples were placed in a refrigerator overnight, the LRW was again changed, and the samples were equilibrated for 2 hr. For final embedding, each segment was removed from the porous vial and placed in a gelatin capsule, with the long axis of the segment rising vertically from the bottom. Fresh LRW was added, and the capsule was capped and placed inside a vacuum desiccator, which was then evacuated slowly to remove any air bubbles in the LRW, backfilled with N_2, and placed in an oven at 60°C for 24 hr to polymerize and harden the LRW.

Throughout the solvent-exchange and resin-infiltration procedures the samples maintained their original color, i.e., oxidized samples were yellow-brown and reduced samples were deep blue-green. The deep blue-green color, which arises from a near maximum in the Fe(II)-Fe(III) intervalence electron transfer transitions (Lear and Stucki, 1987; Komadel *et al.*, 1990), clearly indicates that the reduced sample maintained a significant reduced state (~50%) during this stage of sample preparation.

Thin sections were cut to 500-Å thickness with a diamond knife on a Reichert-Jung Ultracut E microtome using deoxygenated water in the reservoir to prevent reoxidation of the Fe in the clay. To guard further against reoxidation, the entire microtome was placed inside a glove bag specially fitted with surgical gloves and filled with O_2-free N_2 (purged five times). Thin sections were picked up on carbon-coated grids, dried in the glove bag, and transferred immediately to the electron microscope high-vacuum chamber.

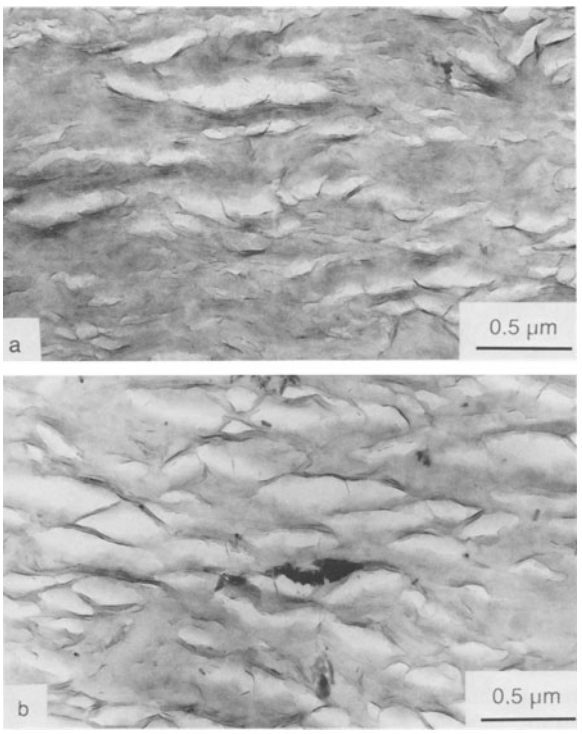

Figure 1. Low-resolution (10,000 ×) transmission electron micrographs showing the particle arrangements in (a) reduced [Fe(II) ~ 0.5 total Fe] and (b) aqueous gels of Na-smectite (SWa-1) equilibrated at 10 kPa.

Electron micrographs at low (10,000 ×) and high (100,000 ×) magnification, energy-dispersive X-ray analysis, and electron diffraction diagrams were obtained using a Philips Model 420 scanning/transmission electron microscope (STEM).

RESULTS AND DISCUSSION

Clay particle arrangements

After equilibration with 10 kPa applied swelling pressure, reduced and oxidized samples consisted of parallel-oriented crystal systems (Figures 1a and 1b). In the oxidized sample some Fe oxide crystals were observed scattered among the clay particles, which is consistent with Murad (1987), who found from Mössbauer spectroscopy that 3% of the Fe in sample SWa-1 was in the form of goethite. The solubilization of finely divided Fe(III) phases by the reducing and chelating actions of dithionite and citrate evidently removed most of the Fe oxide particles from the reduced sample.

In the oxidized sample, HRTEM (Figure 2) showed the extension of particles in the *a-b* plane to be large

https://doi.org/10.1346/CCMN.1991.0390204 Published online by Cambridge University Press

Figure 2. High-resolution (100,000 ×) transmission electron micrographs of oxidized Na-smectite (SWa-1), taken at three different locations on the thin section.

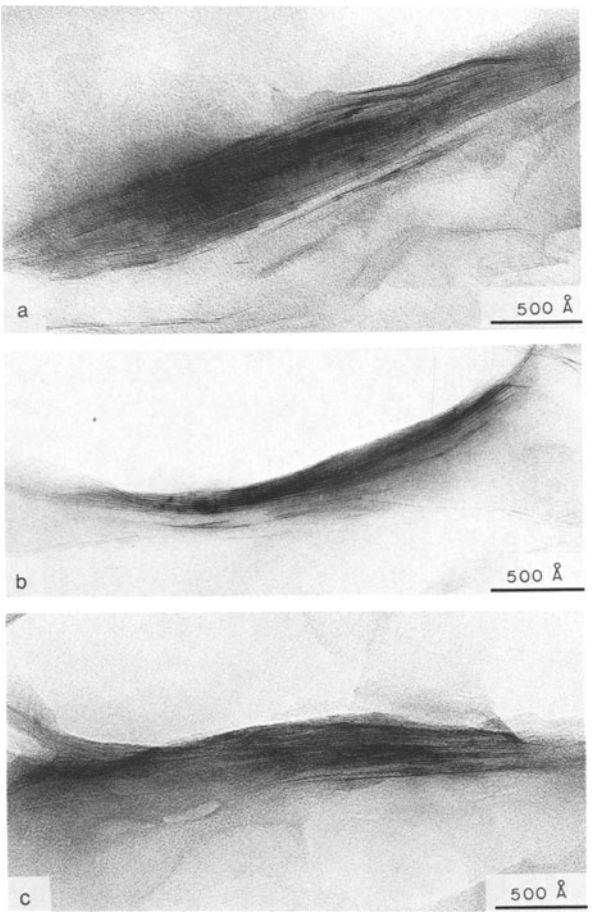

Figure 3. High-resolution (100,000 ×) transmission electron micrographs of reduced Na-smectite (SWa-1), taken at three different locations on the thin section.

compared with the reduced sample, forming a continuous network of small, parallel-oriented crystals. Each crystal consisted of about 1 to 6 layers having 12.6 Å spacings, and the number of total layers in a particle was 10 to 15. Layer spacings >12.6 Å (but <100 Å) probably correspond to slit-shaped pores between adjacent small (1–6 layers) crystals. The reduced sample, on the other hand, consisted of much smaller particles in the *a-b* dimension, extending <2000 Å; but as many as 20 to 40 layers were stacked rather homogeneously along the *c*-axis in the central parts of the particles (Figure 3), exhibiting no variation in layer spacing except a few discontinuities. The reduced system was thus composed of more discrete and more homogeneous particles than found in the network of the oxidized system.

In both the oxidized and reduced systems the overall *c*-axis spacing was similar and close to 12.6 Å. One of the objectives of this study was to differentiate between expanded and collapsed or partially collapsed layers, but the sample preparation methods apparently precluded attainment of this objective. One obvious factor which would have decreased all layer spacings to a common value was the solvent exchange from water to methanol, which represented about a three-fold decrease in the dielectric constant of the suspending medium. The dielectric constant is well-known to have a direct influence on the repulsive forces between two Na-clay layers (van Olphen, 1963). The interlayer distances observed in the LRW-hardened block are thus more representative of a clay-methanol system than of a Na-clay-water system. Annabi-Bergaya *et al.* (1980) and Ben Rhaïem *et al.* (1987) observed a similar phenomenon in low-charge Na-smectite. Studies in which either vermiculite or Ca-smectite was used (e.g., Ben Rhaïem *et al.*, 1987; de la Calle *et al.*, 1976, 1988) would have failed to show an appreciable effect of either methanol or ethanol, because the layers would already have been largely collapsed due to other forces (e.g., presence of divalent cations), leaving the possibility for only a minor influence from the low-dielectric solvents.

Surface area and totally collapsed layers

Although treatment of the layers with methanol explains the absence of fully expanded layers in the electron micrographs, the absence of fully collapsed layers

https://doi.org/10.1346/CCMN.1991.0390204 Published online by Cambridge University Press

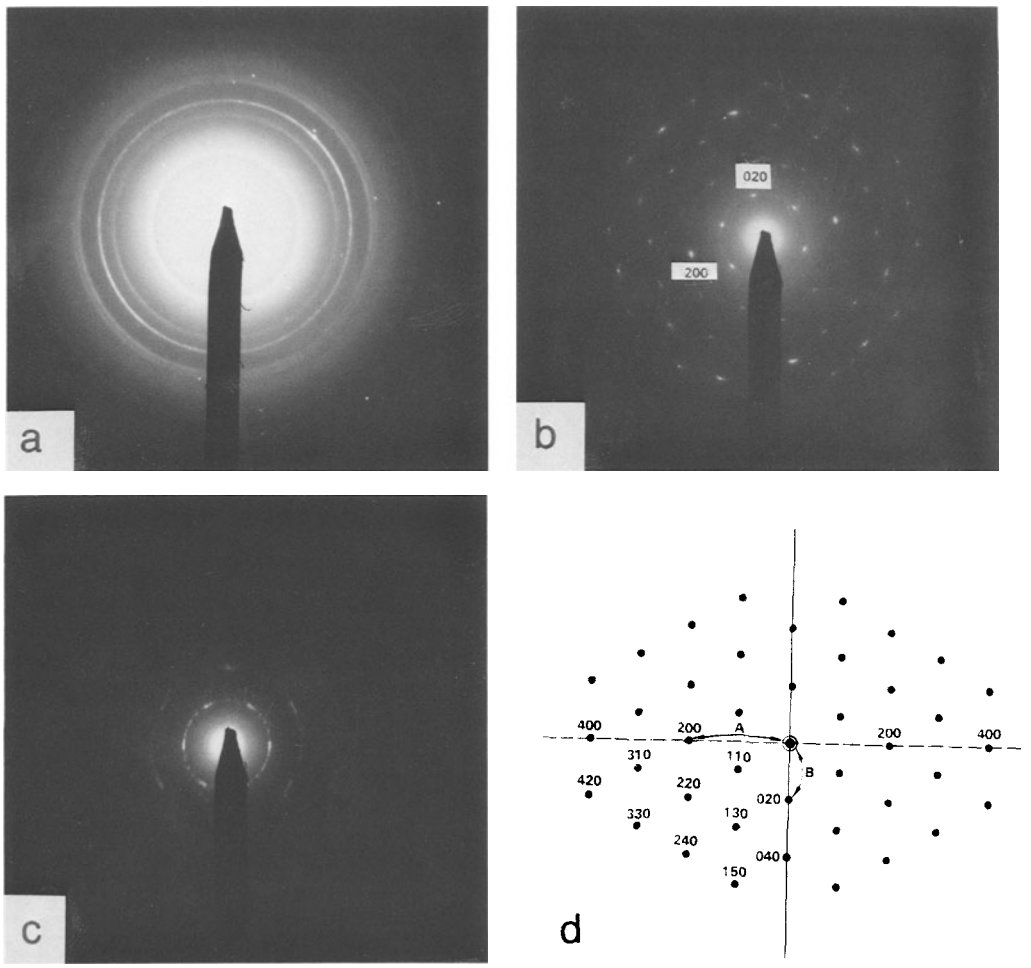

Figure 4. Electron diffraction diagrams: (a) oxidized Na-smectite (SWa-1) gel, (b, c) reduced [Fe(II) ~ 0.5 total Fe] Na-smectite (SWa-1) gel, and (d) theoretical structure.

is more difficult to interpret. Lear and Stucki (1989) observed a significant decrease in EGME adsorption in reduced, compared with oxidized smectite, and thereby deduced a decrease in specific surface area assuming that EGME wets the same inter-laminar surfaces as water. According to Tessier and Pédro (1987), specific surface area is a good indicator of the amount of inter-laminar surface exposed to water in Na-smectite; nevertheless, part of the surface may be inaccessible to relatively neutral molecules such as EGME. In particular, those layers that collapsed to 12.6 Å may exclude EGME, and thus represent the equivalent of completely collapsed layers insofar as this measurement is concerned. But cation fixation, which has been shown for Na^+, K^+, Ca^{2+}, Cu^{2+}, and Zn^{2+} (Chen *et al.*, 1987; Lear and Stucki, 1989; Khaled and Stucki, 1991) to be a result of the reduction of structural Fe, should require more complete collapse of the layers. In the samples used in the present study, about 12% of the interlayer Na^+ is known to be fixed (Lear and Stucki, 1989); but no evidence was found in the electron micrographs of layers significantly more collapsed than 12.6 Å. Perhaps this spacing is sufficient in the case of Na^+ to induce some fixation; however, the results to this point have yet to be fully explained.

Stacking order in the a-b *plane*

Many areas of the samples were examined by electron diffraction to provide an overall statistical view (typical patterns are shown in Figure 4). Smectite is generally regarded as having a turbostratic structure (Méring and Oberlin, 1967; Suquet and Pezerat, 1987), i.e., the rotation of one parallel layer relative to another around the c* axis is completely random or disordered, or, in other words, the stacking order relative to the *a-b* plane is random. The homogeneous rings in the electron diffraction pattern of oxidized sample SWa-1 (Figure 4a) confirm the existence of turbostratic stacking relative to the *a-b* plane. To the contrary, diffraction diagrams from the reduced sample showed discernible

https://doi.org/10.1346/CCMN.1991.0390204 Published online by Cambridge University Press

spots (Figure 4b), in addition to a few low-intensity rings (Figure 4c), which indicate that the sample was more ordered in its face-to-face stacking arrangements than in the oxidized state (Suquet and Pezerat, 1987). This result is rather surprising because layers generally become less ordered as the size of particle increases, but here the opposite effect was observed. Inasmuch as neither the oxidized nor the reduced sample was dried at any stage of the experiment, the stacking order was developed in suspension as a result of increased inter-layer attraction due to the reduction of structural Fe(III) to Fe(II).

Ordered electron diffraction patterns also reveal the *a* and *b* unit-cell edge lengths of the clay crystal. Diffraction spots 200 and 400 give an *a* length for the reduced SWa-1 sample of 5.24 Å, and the 020 and 040 spots give the *b* length as 9.25 Å (Figure 4b). These results can be compared with the theoretical *b* length of dioctahedral smectites, which, according to Brindley and MacEwan (1953), varies with dioctahedral composition according to the equation:

$$b = 8.91 + 0.06x + 0.09q + 0.18r + 0.27s, \quad (1)$$

where x is the tetrahedral Al or Fe(III) content; q, octahedral Fe(III); r, octahedral Mg; and s, octahedral Fe(II). Applying Eq. (1) to sample SWa-1, assuming an oxidized structural formula (Goodman *et al.*, 1976) of

$$Na_{0.328}(Si_{3.65}Al_{0.35})(Al_{0.53}Fe(III)_{1.366}Mg_{0.13})O_{10}(OH)_2, \quad (2)$$

[compensating cation stoichiometry added based on Stucki (1988)] and a reduced structural formula of

$$Na_{0.577}(Si_{3.65}Al_{0.35})(Al_{0.53}Fe(III)_{0.683}Fe(II)_{0.683} \cdot Mg_{0.13})O_{10}(OH)_2, \quad (3)$$

yields theoretical *b* lengths of 9.0773 and 9.2001 Å, respectively. Comparing the latter with the observed value of 9.25 Å for reduced sample SWa-1 suggests reasonably good agreement between theoretical and experimental results. The small difference could be due to the fact that the actual Fe(II) content in the reduced sample was not measured in these experiments, but the value assumed in Eq. (3) is only an estimate based on the reduction time used (Komadel *et al.*, 1990). The maximum theoretical *b* length for a completely reduced sample is 9.323 Å, so if the actual level of reduction is >50%, agreement between theory and experiment would be even better. Some error ($\leq \pm 5\%$) also exists in determining the crystallographic spacings from the electron diffraction patterns, and the Fe in the reduced sample likely existed in some distorted, five-coordinate sites (Lear and Stucki, 1985), the distortions being reflected in the unit cell *b*-edge length.

Due to the presence of rings rather than spots in the electron diffraction patterns of the oxidized sample, the crystallographic parameters were more difficult to deduce. The rings were always thick and diffuse, and the *a*- and *b*-parameters seemed to vary between two extreme values. For the *b* length, the value ranged from 9.05 to 9.24 Å; for *a*, the range was 5.12 to 5.24 Å. The low value for *b* is consistent with a dioctahedral structure and compares well with both the calculated value of 9.0773 Å from Eq. (1) and the value of 9.07 Å observed by Russell and Clark (1978). The higher value is typical of a trioctahedral clay. The possibility that rings from certain diffracting positions overlapped, especially the 020 and 110, 130 and 200, 040 and 220, and 060 and 330 reflections (Eberhart, 1976), introduces sufficient uncertainty to prevent the use of these electron diffraction results alone to determine whether the oxidized structure is di- or trioctahedral. Based on the octahedral cation composition of 2.025 reported by the structural formula [Eq. (2)], however, the clay is probably not trioctahedral.

Chemical analysis

Energy-dispersive X-ray analyses of oxidized and reduced thin sections failed to reveal a qualitative difference in chemical composition between the two sample treatments. Figure 5 shows two diagrams from the reduced sample, which differ slightly in overall intensities, but which were virtually identical within the resolution of the measurements. No qualitative differences were found between results from oxidized and reduced samples. More refined, quantitative elemental analysis will be required to reveal whether any such differences occur as a result of Fe reduction and oxidation.

SUMMARY AND CONCLUSIONS

Transmission electron microscopy measurements showed that the texture, particle size, and interlayer distances of ferruginous smectite SWa-1 were markedly altered by the oxidation state of structural Fe. Even though the sample preparation technique precluded observation of fully expanded layers, the results revealed that the oxidized sample consisted of small (1–6 layers) crystal units interconnected in a large network, typical of low-charge smectite. The reduced sample, by contrast, consisted of thicker (20–40 layers), more distinct particles, which were limited in lateral extent to about 2000 Å. The interlayer distance of the reduced sample was more uniform (12.6 Å) than for the oxidized sample.

Because cohesion forces between oxidized clay layers are weaker than between reduced layers (Stucki *et al.*, 1984a; Lear and Stucki, 1989; Khaled and Stucki, 1991), adjacent oxidized layers glide more easily over one another, are more easily curved, and thus form thin but relatively long ribbons. Conversely, the greater attraction between reduced layers inhibits lateral crystal growth while promoting thicker stacks of layers, which are more ordered in the *a*-*b* dimension.

Electron diffraction patterns showed that the stack-

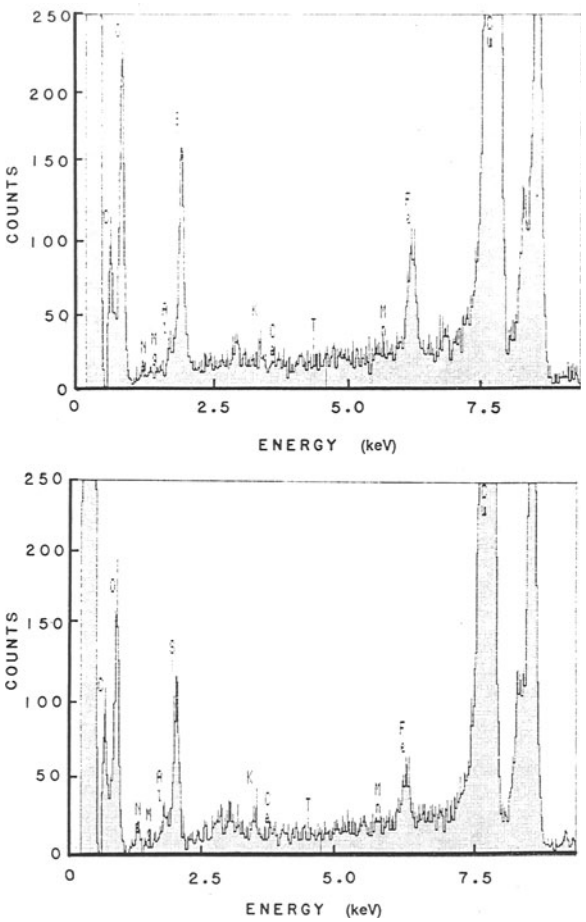

Figure 5. Energy-dispersive X-ray spectra of reduced [Fe(II) ≥ 0.5 total Fe] Na-smectite (SWa-1) gel. (a) and (b) represent two, randomly-selected locations on the grid.

ing order of the oxidized sample was turbostratic, whereas much more order was present in the reduced sample. These results offer further evidence that the presence of Fe(II) in the crystal structure of smectites increases the attractive forces between clay layers and suggest that Fe(II) may have a unique influence on the surface chemistry of clays. Still unknown, however, is the precise distribution of interlayer distances that were present in the reduced and oxidized smectite gels, in various stages of wetting and drying. Low-angle X-ray scattering measurements are currently underway to measure these spacings directly.

ACKNOWLEDGMENTS

The authors gratefully acknowledge the assistance of Theresa C. Wilkinson, who prepared the embedded samples, and the financial support of this project by the Illinois Agricultural Experiment Station, the Institut National de la Recherche Agronomique (INRA), and the NATO Collaborative Research Grants Program.

REFERENCES

Annabi-Bergaya, F., Cruz, M. I., Gatineau, L., and Fripiat, J. J. (1980) Adsorption of alcohols by smectites. Role of exchangeable cations: *Clay Miner.* **15,** 219–233.

Ben Rhaïem, H., Pons, C. H., and Tessier, D. (1987) Factors affecting the microstructure of smectites: Role of cation and history of applied stresses: in *Proc. Int. Clay Conf. Denver, 1985,* L. G. Schultz, H. van Olphen, and F. A. Mumpton, eds., The Clay Minerals Society, Bloomington, Indiana, 292–297.

Brindley, G. W. and MacEwan, D. M. C. (1953) Structural aspects of the mineralogy of clays and related silicates: in *Ceramics: A Symposium,* A. T. Green and G. H. Stewart, eds., The British Ceramic Society, London, 15–59.

de la Calle, C., Dubernat, J., Suquet, H., Pezerat, H., Gaultier, J. P., and Mamy, J. (1976) Crystal structure of two layer Mg-vermiculites and Na-, Ca-vermiculites: in *Proc. Int. Clay Conf., Mexico City, 1975,* S. W. Bailey, ed., Applied Publishing, Wilmette, Illinois, 201–209.

de la Calle, C., Suquet, H., and Pons, C. H. (1988) Stacking order in a 14.30-Å Mg-vermiculite: *Clays & Clay Minerals* **36,** 481–490.

Chen, S. Z., Low, P. F., and Roth, C. B. (1987) Relation between potassium fixation and the oxidation state of octahedral iron: *Soil Sci. Soc. Amer. J.* **41,** 82–86.

Eberhart, J. P. (1976) *Methodes Physiques d'Etude des Mineraux et des Materiaux Solides:* Doen, Paris, 507 pp.

Goodman, B. A., Russell, J. D., Fraser, A. R., and Woodhams, F. W. D. (1976) A Mössbauer and I.R. spectroscopic study of the structure of nontronite: *Clays & Clay Minerals* **24,** 53–59.

Khaled, E. M. and Stucki, J. W. (1991) Effects of iron oxidation state on cation fixation in smectites: *Soil Sci. Soc. Amer. J.* **55,** (in press)

Komadel, P., Lear, P. R., and Stucki, J. W. (1990) Reduction and reoxidation of iron in nontronites: Rate of reaction and extent of reduction: *Clays & Clay Minerals* **37,** 203–208.

Lear, P. R. and Stucki, J. W. (1985) Role of structural hydrogen in the reduction and reoxidation of iron in nontronite: *Clays & Clay Minerals* **33,** 539–545.

Lear, P. R. and Stucki, J. W. (1987) Intervalence electron transfer and magnetic exchange in reduced nontronite: *Clays & Clay Minerals* **35,** 373–378.

Lear, P. R. and Stucki, J. W. (1989) Effects of iron oxidation state on the specific surface area of nontronite: *Clays & Clay Minerals* **37,** 547–552.

Méring, J. and Oberlin, A. (1967) Electron-optical study of smectites: in *Clays and Clay Minerals, Proc. 15th Natl. Conf., Pittsburgh, Pennsylvania, 1966,* S. W. Bailey, ed., Pergamon Press, New York, 3–25.

Murad, E. (1987) Mössbauer spectra of nontronites: Structural implications and characterization of associated iron oxides: *Z. Pflanzernähr. Bodenk.* **150,** 279–285.

Russell, J. D. and Clark, D. R. (1978) The effect of Fe-for-Si substitution on the *b*-dimension of nontronite: *Clay Miner.* **13,** 133–138.

Stucki, J. W. (1988) Structural iron in smectites: in *Iron in Soils and Clay Minerals,* J. W. Stucki, B. A. Goodman, and U. Schwertmann, eds., D. Reidel, Dordrecht, The Netherlands, 625–675.

Stucki, J. W., Golden, D. C., and Roth, C. B. (1984a) The preparation and handling of dithionite-reduced smectite suspensions: *Clays & Clay Minerals* **32,** 191–197.

Stucki, J. W., Low, P. F., Roth, C. B., and Golden, D. C. (1984b) Effects of oxidation state of octahedral iron on clay swelling: *Clays & Clay Minerals* **32,** 357–362.

Stucki, J. W. and Lear, P. R. (1989) Variable oxidation states of iron in the crystal structure of smectite clay minerals: in *Structures and Active Sites of Minerals,* L. M. Coyne, D.

Blake, and S. McKeever, eds., American Chemical Society, Washington, D.C., 330–358.

Suquet, H. and Pezerat, H. (1987) Parameters influencing layer stacking types in saponite and vermiculite: A review: *Clays & Clay Minerals* **35,** 353–362.

Tessier, D. (1984) Etude experimentale de l'organisation des materiaux argileux: Hydratation, gonflement et structuration au cours de la dessiccation et de la réhumectation: Ph.D. thesis, University of Paris VII, Paris, 361 pp.

Tessier, D. and Pédro, G. (1987) Mineralogical characterization of 2:1 clays in soils: Importance of the clay texture: in *Proc. Int. Clay Conf., Denver, 1985,* L. G. Schulze, H. van Olphen, and F. A. Mumpton, eds., The Clay Minerals Society, Bloomington, Indiana, 78–84.

van Olphen, H. (1963) *An Introduction to Clay Colloid Chemistry:* Wiley, New York, 251–270.

Wu, J., Low, P. F., and Roth, C. B. (1989) Effects of octahedral-iron reduction and swelling pressure on interlayer distances in Na-nontronite: *Clays & Clay Minerals* **37,** 211–218.

(Received 19 April 1990; accepted 6 July 1990; Ms. 2002)